Detection of chemical warfare agents based on quantum cascade laser cavity ring-down spectroscopy

Zhechao Qu (曲哲超)[1,2], Chunming Gao (高椿明)[3], Yanling Han (韩艳玲)[1], Xiaosong Du (杜晓松)[3], and Bincheng Li (李斌成)[1*]

[1] *Institute of Optics and Electronics, Chinese Academy of Sciences, Chengdu 610209, China*

[2] *Graduate University of Chinese Academy of Sciences, Beijing 100049, China*

[3] *School of Optoelectronic Information, University of Electronic Science and Technology of China, Chengdu 610054, China*

[*] *Corresponding author: bcli@ioe.ac.cn*

Received August 30, 2011; accepted November 30, 2011; posted online January 17, 2012

Chemical warfare agents (CWAs) are recognized as serious threats of terrorist acts against the civilian population. Minimizing the impact of these threats requires early detection of the presence of CWAs. Cavity ring-down spectroscopy (CRDS) is an exquisitely sensitive technique for the detection of trace gaseous species. In this letter, the CRDS technique is employed using a pulsed quantum cascade laser for the detection of dimethyl methylphosphonate (DMMP). A limit of DMMP detection of approximately 77 ppb is achieved. The best achievable sensitivity that corresponds to noise-equivalent absorption is approximately 2×10^{-7}cm^{-1}.

OCIS codes: 010.1030, 140.5965, 300.6270.

doi: 10.3788/COL201210.050102.

The need for detection of chemical warfare agents (CWAs) is no longer confined to battlefield environments; at least one confirmed terrorist attack occurred in the Tokyo Subway in 1995. Most CWAs are nerve agents, e.g., Tabun (GA), Sarin (GB), Soman (GD), CycloSarin (GF), and Triethyl phosphate (TEP)[1]. These nerve agents pose a very challenging menace in homeland security due to their very low lethal concentrations. Researchers have taken to the task of identifying and working with non- or slightly toxic simulant chemical compounds that exhibit similar molecular features to highly toxic nerve agents. As a result, a series of simulant materials have been identified, exhibiting similar vibrational-rotational molecular behaviors of CWAs[2]. One of the most commonly known simulant nerve agents is dimethyl methylphosphonate (DMMP), which is chosen as the stimulant in the present experiments.

Infrared (IR) absorption spectroscopy has been widely investigated and applied for the detection of trace gases and vapors. The long path absorption measurements of cavity ring-down spectroscopy (CRDS)[3] and the calorimetric techniques of photoacoustic spectroscopy (PAS)[4] are two common absorption spectroscopy-based techniques for high sensitivity detection of gaseous molecules. CRDS techniques provide a long path length on the order of several kilometers in a small effective volume[5]. Additionally, CRDS measurement results are independent of the laser intensity fluctuation[6]. These features are attractive for trace CWAs monitoring in real time.

Quantum cascade lasers (QCLs) are now commercially available in continuous wave (CW) and pulsed modes of operation[7]. QCLs operating in the mid- and long-wave IR region (3–24 μm) enable direct access to the vibrational-rotational bands of most molecular species[8]. A number of trace gas sensors with high sensitivity have been developed based on QCLs. The ability of detecting trace gases in real time at ppm to ppb levels is of great interest in the fields of environmental science, homeland security, medical diagnostics, among others[9,10].

In this letter, the CRDS technique using a tunable long-wave IR distributed feedbackpulsed QCL is employed for the detection of trace CWAs. Baseline noise level in the QCL-CRDS experiment yields a noise-equivalent absorption limit of approximately 2×10^{-7}cm^{-1}, independent of the absorbing medium. By detecting the spectroscopic features of DMMP, the limit of detection of approximately 77 ppb is achieved. Based on this QCL-CRDS setup, projected detection limits for several CWAs (e.g., GA, GB, GD, GF, TEP, and diisopropyl methylphosphonate (DIMP)) are presented.

A schematic diagram of the experimental setup is shown in Fig. 1. A pulsed distributed feedback QCL operating near 9.7 μm (SB13, Alpes Lasers) is employed as the light source. The QCL is mounted in a Peltier-cooled laboratory laser housing. The laser pulsed duration and repetition rate are controlled by a QCL pulser timing unit. A temperature controller is used to tune and control the laser temperature. A DC power supply and a QCL pulse switching unit provide the laser driving current.

The laser wavenumber, as a function of the heat sink

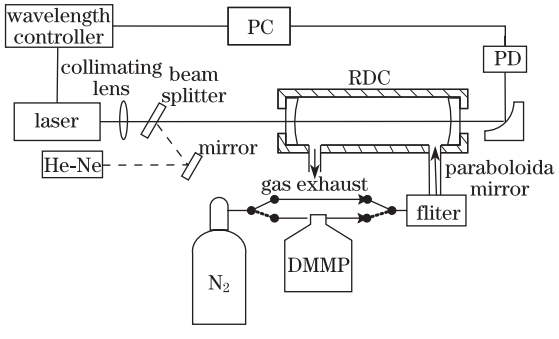

Fig. 1. Schematic diagram of the apparatus for the QCL-CRDS experiment.

temperature, is shown in Fig. 2(a). By changing the temperature with the temperature controller, the laser frequency is tuned to a rate of 0.07187 cm^{-1}/K. The output power of the laser as a function of wavenumber is shown in Fig. 2(b); the laser pulse repetition rate is set to 200 kHz, which is below the critical maximum of 2% of the duty cycle of the laser at the pulse duration of 40 ns. The laser output power increases with the increasing wavenumber, whereas the full temperature tuning range is between −30 and 30 °C. Experimentally, the laser heat sink temperature is scanned from −30 to 15 °C (wavenumber from 1 027.67 to 1 024.44 cm^{-1}) as the signal-to-noise ratio (SNR) of the ring-down signals decreases with the increasing temperature.

The laser beam from the QCL is highly divergent with a large axis angle (full-width at half-maximum (FWHM): 60° × 40°). Thus, an antireflection coated aspheric ZnSe lens with a focal length of 12 mm and a clear aperture of 15 mm is used to collimate the laser beam. The collimated laser light is directed into the ring-down cavity (RDC). The RDC consists of two highly reflective plano-concave mirrors (R >99.9% at 9.7 μm) with curvature radius of −100 cm and diameter of 25.4 mm. The RDC length is 50 cm. The ring-down signals are monitored by detecting the laser beam that leaks out of the rear mirror of the RDC. This light is focused by an off-axis paraboloidal reflector onto a liquid nitrogen-cooled HgCdTe photoconductive detector (KMPV 11-1-J1/DC, Kolmar, rise time 2.5 ns) for detection. A He-Ne laser is used to facilitate alignment of the optical components.

The molecules of CWAs have their strong fundamental absorption lines in the longwave IR region between 9.0 and 11.5 μm as shown in Fig. 3; the spectral data are from the Pacific Northwest National Laboratory (PNNL)[11]. The absorption features of CWAs are very broad, making the detection of these CWAs easy even with non-tunable lasers. In the range of 9.73−9.76 μm, the absorbance of DMMP is between 0.20×10^{-5} and 0.26×10^{-5} cm^{-1}/ppm.

In the CRDS technique, the recorded CRDS signals are fitted to an exponential decay function to extract the ring-down time. The RDC total loss, combining the background loss and sample absorption loss, is given by $\alpha_{\rm loss}(\lambda)=1/c\tau(\lambda)$, where c is the speed of light and $\tau(\lambda)$ is the ring-down time at the wavelength λ. The background

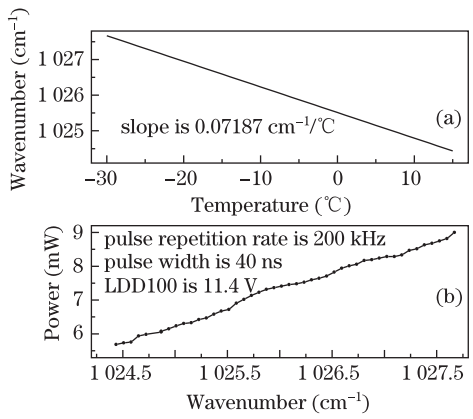

Fig. 2. (a) Temperature tuning of the QCL and (b) QCL power as a function of the wavenumber.

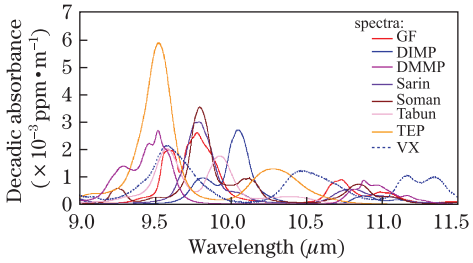

Fig. 3. (Color online)Absorption features of CWAs in the 9.0–11.5 μm region.

loss of the sample cell is subtracted to obtain the spectrum of the trace gas sample. By recording the difference of $\alpha_{\rm loss}(\lambda)$ as a function of the wavelength, the absorption spectrum of the sample under investigation can be obtained.

In the experiments, the ambient temperature is 25 °C, and the pressure in the sample cell is constant at 1 atm. The baselines shown in Fig. 4(a) (lower lines) are obtained with the high purity nitrogen flowing through the sample cell. Two baselines are measured before the DMMP is injected into the sample cell and after 10 min of nitrogen flushing after DMMP detection, respectively. The baseline loss in the case of pure nitrogen flow is invariable over the entire scan range at the value of approximately 1.55×10^{-5} cm^{-1}, attributable to the transmission loss of the RDC mirrors. The reflectance of the RDC mirrors of 99.92% can be calculated by the baseline loss. Figure 4(a) (upper line) shows the observed spectrum pattern of the DMMP together with the baseline loss. Two absorption peaks of DMMP centered at approximately 1 025.8 and 1 027.3 cm^{-1} can be observed in the scanned spectral range. Correspondingly, the absolute absorption loss of DMMP is presented in Fig. 4(b). Given that the spectrum width of the QCL is much narrower than that of the absorption peak of the DMMP, the laser linewidth effect on the absorption loss measurement can be neglected[12]. The concentration of DMMP can be easily calculated via $C=\alpha_{\rm absorb}(\lambda)/\alpha_{\rm PNNL}(\lambda)$, with $\alpha_{\rm absorb}(\lambda)$ and $\alpha_{\rm PNNL}(\lambda)$ representing the measured absorption loss and the absorbance in the PNNL database at the wavelength λ, respectively. The concentration of DMMP shown in Fig. 4(b) is approximately 5.4 ppm.

The measured DMMP absorption loss, as a function of DMMP concentration from approximately 630 ppb to 14.3 ppm, is shown in Fig. 5. The concentration of DMMP is calculated by both absorption peaks of DMMP centered at 1 025.8 and 1 027.3 cm^{-1}, respectively. The concentrations calculated by both absorption peaks are in good agreement. In the QCL-CRDS experiment, the noise-equivalent absorption limit is approximately $2\times10^{-7}cm^{-1}$, estimated from the observed 3σ baseline noise and corresponding to the limit of DMMP detection of approximately 77 ppb. The sensitivity of the apparatus can be improved by employing a QCL with higher power, or constructing an RDC with a longer ring-down time.

For a CWA-detection apparatus, the required sensitivity for CWA detection is determined by the toxicity levels of particular agents[13]. The lethal concentrations for 10 min of exposure and projected sensitivity of GA, GB, GD, and GF are summarized in Table 1, based on

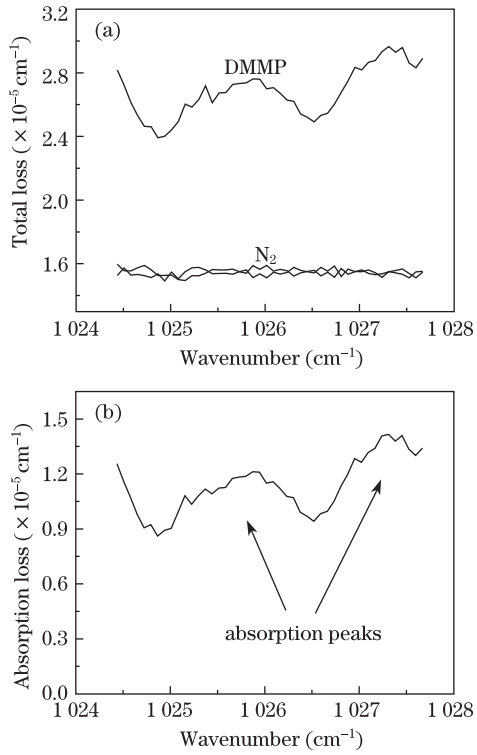

Fig. 4. (a) The total loss of the RDC. The upper and lower lines indicate the sample cell filled with mixed gas of DMMP and N_2 and with N_2 only, respectively; (b) the measured absorption spectrum of DMMP at 1 atm; the concentration of DMMP is approximately 5.4 ppm.

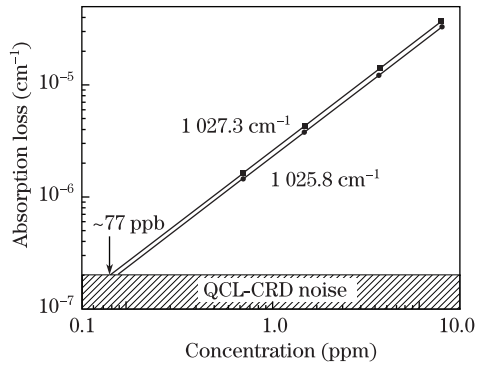

Fig. 5. Measured absorption loss as a function of DMMP concentration, showing a noise limited minimum detection level of 77 ppb.

Table 1. Lethality Concentration and Projected Detection Limits for Several CWAs based on QCL-CRDS Results

Species	9.73–9.76 μm max absorbance (cm^{-1}/ppm)	Lethality 10 min (ppb)	Detection (ppb)
DMMP	0.26	$> 10^5$	77
DIMP	0.8	$> 10^5$	25
TEP	0.8	$> 10^5$	25
GA	0.7	100	26.4
GB	3.0	64	6.7
GD	3.2	49	6.3
GF	2.5	53	8.0

the QCL-CRDS instrumental sensitivity of 2×10^{-7}cm^{-1}. Considering the lower projected sensitivities compared with the lethal concentrations, the experimental apparatus has the potential for CWAs alarm.

Currently, the PAS technique has been the most commonly used for the measurement of CWAs at low concentrations. To date, the minimum detection limit of DMMP is 0.5 ppb using a widely tunable external grating cavity QCL-based PAS technique[14]. In the present QCL-CRDS experimental scheme, the sensitivity can be greatly improved as follows: (1) the sensitivity can be enhanced approximately one order of magnitude by measuring DMMP at the absorption peak rather than at the wing band spectrum measured in the current experiment; (2) the sensitivity can also be increased by constructing a RDC with a longer ring-down time, e.g., increasing the reflectance of the cavity mirrors or extending the RDC length; (3) the SNR of the apparatus decreases as the reflectance of the cavity mirrors increases; the SNR can be increased by improving the power of the light source and the sensitivity of the detector or employing a more sensitive detection method.

In conclusion, a high sensitivity detection of DMMP is demonstrated employing the QCL-CRDS technique. The absorption spectrum of DMMP in the range of 9.73−9.76 μm is measured. A limit of DMMP detection of approximately 77 ppb is experimentally achieved corresponding to the noise-equivalent absorption of 2×10^{-7} cm^{-1}.

This work was supported by the National Natural Science Foundation of China under Grant No. 60878038.

References

1. M. E. Webber, M. Pushkarsky, and C. K. N. Patel, Proc. SPIE **5617,** 34 (2004)
2. K. P. Gurton, M. Felton, R. Dahmani, and D. Ligon, Appl. Opt. **46,** 6323 (2007).
3. A. O'Keefe and D. A. G. Deacon, Rev. Sci. Instrum. **59,** 2544 (1988).
4. M. B. Pushkarsky, M. E. Webber, and C. K. N. Patel, Appl. Phys. B **77,** 381 (2003).
5. I. Debecker, A. K. Mohamed, and D. Romanini, Opt. Express **13,** 2906 (2005).
6. D. Romanni, M. Chenevier, S. Kassi, M. Schmidt, C. Valant, M. Romonet, J. Lopez, and H.-J. Jost, Appl. Phys. B **83,** 659 (2006).
7. W. Guo, J. Liu, J. Chen, L. Li, L. Wang, F. Liu, and Z. Wang, Chin. Opt. Lett. **9,** 061404 (2011).
8. G. N. Rao and A. Karpf, Appl. Opt. **50,** A100 (2011).
9. J. Hildenbrand, J. Herbst, J. Wollenstein, and A. Lambrecht, Proc. SPIE **7222,** 72220B (2009).
10. T. H. Risby and S. F. Solga, Appl. Phys. B **85,** 421 (2006).
11. T. J. Johnson, R. L. Sams, and S. W. Sharpe, Proc. SPIE **5269,** 159 (2004).
12. P. Zalicki and R. N. Zare, J. Chem. Phys. **102,** 2708 (1995).
13. National Research Council (NRC) Volume 3, Acute Exposure Guidelines for Selected Airborne Chemicals (National Academy Press, 2003).
14. A. Mukherjee, I. Dunayevskiy, M. Prasanna, R. Go, A. Tsekoun, X. Wang, J. Fan, and C. K. N. Patel, Appl. Opt. **47,** 1543 (2008).